



Department of Digital Business

**Journal of Artificial Intelligence and Digital Business (RIGGS)**

Homepage: <https://journal.ilmudata.co.id/index.php/RIGGS>

Vol. 4 No. 4 (2026) pp: 15327-15334

P-ISSN: 2963-9298, e-ISSN: 2963-914X

---

## Numerical Optimization of Electric Field Characteristics in FGM Solid Insulators

Satia Zaputra<sup>1</sup>, Usman Sartoyo<sup>2</sup>, Yudhi Hermawan<sup>3</sup>

<sup>1,2,3</sup>Department of Electrical Engineering, Faculty of Industrial Technology, National University of the Republic of Indonesia

[satiazaputra@fti.ukri.ac.id](mailto:satiazaputra@fti.ukri.ac.id)

### Abstract

*Electric field concentration in solid insulation is a critical issue because it can accelerate dielectric degradation, reduce insulation reliability, and increase the possibility of local electrical stress in high-voltage applications. Functionally graded material (FGM) has been widely investigated as an effective method for electric field grading through controlled spatial permittivity distribution. This study aims to optimize the electric field characteristics of FGM solid insulators using a numerical simulation approach. A cylindrical coaxial insulator model consisting of a central high-voltage conductor and five concentric dielectric layers was analyzed under three relative permittivity configurations, namely homogeneous, small-big (SB), and big-small (BS). The simulation was carried out at an applied voltage of 150 kV, and the performance of each configuration was evaluated using the maximum electric field, minimum electric field, average electric field, and electric field grading index. The results show that the permittivity distribution significantly affects the radial electric field profile and local field enhancement in critical regions. The BS-type FGM exhibited the best performance, with the lowest maximum electric field of 3.741 kV/mm and the highest electric field grading index of 81.25%, compared with 5.099 kV/mm and 58.85% for the homogeneous insulator, and 6.921 kV/mm and 42.78% for the SB-type FGM. These findings confirm that numerical simulation is effective for identifying suitable FGM configurations to reduce electric field concentration and improve field grading performance in solid insulators.*

**Keywords:** FGM Solid Insulator, Electric Field Distribution, Numerical Simulation, Electric Field Grading, Permittivity Optimization

### 1. Introduction

The continuous development of high-voltage power equipment has led to increasing demands for compact insulation structures that can operate safely under higher electric stress. In such systems, solid insulators play a critical role because their electrical performance strongly influences insulation reliability and service life. In gas-solid insulation structures, electric field concentration around the spacer remains one of the main design challenges, especially near the interface between the conductor, solid insulator, and surrounding gas [1], [2].

A major problem in solid insulation design is the non-uniform electric field distribution that causes local stress enhancement in critical regions. In GIS-type configurations, field intensification is commonly observed near the high-voltage triple junction, where the spacer, gas medium, and electrode meet. This region is often regarded as the weakest point of the insulation system because excessive local electric stress may accelerate insulation degradation and reduce breakdown strength. Conventional approaches for field control, such as spacer shape modification, additional shielding, and geometric optimization, can reduce field distortion, but they usually increase structural complexity and manufacturing cost [6], [9].

To overcome these limitations, many researchers have proposed the use of Functionally Graded Material (FGM) as an alternative electric field grading technique. FGM is characterized by a spatial distribution of dielectric permittivity and, in some cases, conductivity, allowing the electric field to be redistributed inside and around the solid insulation. This concept enables the reduction of electric field concentration while maintaining a relatively simple insulator geometry. Earlier studies have shown that FGM can be applied to GIS spacers, cone-type insulators, disk-type insulators, and other gas-insulated apparatus through numerical simulation and material engineering approaches [1], [3], [13].

The effectiveness of permittivity-graded materials has been demonstrated in both simulation and fabrication studies. Kurimoto et al. showed that suitable permittivity grading can reduce electric stress on electrode surfaces and improve long-term insulation performance, while Ishiguro et al. reported that a coaxial disk-type FGM could reduce the maximum electric field at the HV-electrode/spacer interface compared with a uniform insulator [7], [6]. In addition, practical fabrication methods such as flexible mixture casting have been developed to realize  $\epsilon$ -FGM structures with controlled permittivity distributions, indicating that field grading by material design is not only theoretically attractive but also manufacturable [8], [13], [15].

Further studies also revealed that electric field relaxation by FGM is closely related to insulation performance improvement. Cone-type and truncated cone-type  $\epsilon$ -FGM spacers fabricated for gas-insulated applications showed reduced electric field intensity and improved discharge inception or breakdown voltage in SF<sub>6</sub> gas [4], [8], [13]. These findings confirm that suppressing the maximum electric field in critical regions is a practical and meaningful indicator for evaluating insulation design.

Besides AC and impulse applications, recent studies have extended the FGM concept to DC insulation systems by introducing combinations of graded permittivity and conductivity. These works indicate that electric field control depends on the dominant material property under each operating condition: permittivity under AC or impulse stress, conductivity under DC steady state, and both properties under transient DC conditions [1], [3]. Although the present study focuses on electric field optimization under a numerical electrostatic framework, these previous findings further support the broader relevance of FGM as a field grading strategy for advanced insulation systems.

In practical design, numerical simulation has become one of the most effective tools for analyzing electric field behavior in solid insulation. The Finite Element Method (FEM) is widely used because it can handle complex geometries, multi-layer dielectric arrangements, and electric field evaluation along critical paths. Previous FGM spacer studies have successfully employed FEM-based simulation to compare different permittivity distributions and to identify configurations that produce lower peak electric stress and more uniform field profiles [9], [10], [12]. This makes simulation-based optimization highly suitable for the preliminary design and evaluation of FGM solid insulators.

Although the existing literature has clearly established the potential of FGM for electric field grading, the optimal behavior of discrete radial permittivity arrangements in a cylindrical coaxial solid insulator still deserves further investigation. In particular, a direct comparison among a homogeneous insulator and stepwise FGM arrangements such as small-big (SB) and big-small (BS) distributions is important to clarify how the direction of permittivity grading influences the maximum electric field, the average field level, and the field uniformity along the radial path. This issue is especially relevant for simple multilayer FGM structures that are easier to model and potentially easier to fabricate than fully continuous gradients [5], [11], [15].

Therefore, this study aims to optimize the electric field characteristics of an FGM solid insulator by numerical simulation. A cylindrical coaxial model with five concentric dielectric layers is used to compare three configurations, namely homogeneous insulation, SB-type FGM, and BS-type FGM. The evaluation is carried out based on the maximum electric field, minimum electric field, average electric field, and electric field grading index. The main contribution of this work is to provide a clear comparative analysis of how discrete permittivity grading affects electric field concentration in critical regions and to identify the most effective FGM configuration for improving field uniformity in solid insulators.

## 2. Research Methods

This study employed a numerical simulation approach to evaluate the electric field characteristics of a solid insulator based on Functionally Graded Material (FGM). The main objective was to identify the permittivity distribution configuration that can reduce the maximum electric field in critical regions and improve the overall electric field uniformity. Numerical simulation was selected because it is widely used for analyzing electric field behavior in multilayer insulation structures and for comparing alternative dielectric designs before fabrication [9], [10], [12].

### 2.1. Geometry of the Solid Insulator Model

The solid insulator was modeled using a cylindrical coaxial geometry. In this configuration, the high-voltage conductor was located at the center of the insulator structure, while the outer boundary represented the grounded

region. The inner diameter of the insulator was 60 mm and the outer diameter was 160 mm, resulting in a total radial insulation thickness of 100 mm. To implement the FGM concept, the dielectric region was divided into five concentric layers of equal thickness. Each layer had a radial thickness of 10 mm, forming a five-layer discrete permittivity grading structure.

Figure 1 presents the cylindrical coaxial geometry of the discrete permittivity-graded FGM solid insulator used in the numerical simulation. The model comprises a central HV conductor and five concentric dielectric layers with different relative permittivities, forming a symmetrical radial grading structure. The critical regions near the triple junctions, denoted as TJ-HV and TJ-GND, are also identified because they are associated with electric field concentration.

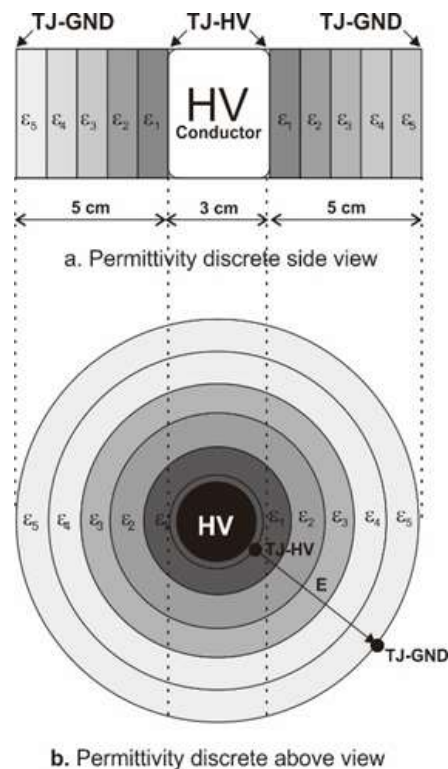


Figure 1. Geometry of the discrete permittivity-graded FGM solid insulator: (a) side view and (b) top view.

The cylindrical coaxial geometry was selected because it provides a clear radial electric field profile and allows direct comparison of electric field redistribution under different dielectric arrangements. This geometry is also relevant for spacer-type solid insulation systems used in gas-insulated structures [2], [6], [10].

## 2.2. Permittivity Distribution Configurations

Three dielectric configurations were investigated in this study, namely homogeneous insulation, small-big (SB)-type FGM, and big-small (BS)-type FGM. In the homogeneous configuration, all dielectric layers were assigned the same relative permittivity. In contrast, the FGM configurations employed stepwise permittivity variation across the five concentric layers.

Table 1 summarizes the relative permittivity distribution used for each dielectric configuration. In the homogeneous model, all five layers were assigned the same relative permittivity of 3.5. In contrast, the BS-type FGM employed a decreasing permittivity distribution from 7.5 to 3.5 along the radial direction, whereas the SB-type FGM used an increasing distribution from 3.5 to 7.5. These stepwise arrangements were defined to examine how the direction of permittivity grading affects electric field redistribution and field concentration in the solid insulator.

Table 1. Relative permittivity distribution for the homogeneous and FGM solid insulator configurations.

Configuration	$\epsilon_1$	$\epsilon_2$	$\epsilon_3$	$\epsilon_4$	$\epsilon_5$
Homogeneous	3.5	3.5	3.5	3.5	3.5
BS-type FGM	7.5	6.5	5.5	4.5	3.5
SB-type FGM	3.5	4.5	5.5	6.5	7.5

In the SB-type FGM, the relative permittivity increased gradually from the inner region near the high-voltage conductor toward the outer region. In the BS-type FGM, the relative permittivity decreased gradually from the inner region toward the outer region. These two grading schemes were selected to evaluate the influence of grading direction on electric field redistribution and field concentration reduction. Previous studies have shown that the arrangement of permittivity gradients strongly affects the field intensity near high-stress regions and determines the effectiveness of field grading [1], [3], [7].

### 2.3. Simulation Condition

The numerical simulation in this study was carried out based on the electrostatic field formulation. The electric field intensity,  $E$ , was obtained from the negative gradient of the electric potential,  $V$ , as expressed in (1). Meanwhile, the electric potential distribution in the dielectric region was governed by Gauss's law for electrostatics, as given in (2), where  $\epsilon_0$  is the vacuum permittivity,  $\epsilon_r$  is the relative permittivity of the material, and  $\rho_v$  is the volume charge density. These equations were used as the fundamental basis for evaluating the electric field distribution in the multilayer FGM solid insulator model.

$$E = -\nabla V \quad (1)$$

$$\nabla \cdot (\epsilon_0 \epsilon_r E) = \rho_v \quad (2)$$

The electric field simulation was carried out under an applied voltage of 150 kV. The electric field magnitude along the radial direction of the insulator was extracted as the main simulation output. The radial observation path extended from the inner side of the solid insulator near the high-voltage conductor to the outer side near the grounded region. The simulation results were expressed in kV/mm for easier engineering interpretation. This unit was selected because it allows direct comparison with common dielectric strength references of gaseous insulation media, such as air and SF<sub>6</sub>.

### 2.4. Electric Field Evaluation Parameters

The performance of each dielectric configuration was evaluated using four main parameters, namely the maximum electric field ( $E_{max}$ ), minimum electric field ( $E_{min}$ ), average electric field ( $E_{avg}$ ), and electric field grading index ( $\eta$ ).

The maximum electric field represents the highest local electric stress along the radial path and is used as the main indicator of field concentration in the critical region. The minimum electric field represents the lowest electric stress within the evaluated region. The average electric field was obtained from the radial electric field profile to describe the overall field level in the insulator.

$$\eta = (E_{avg} / E_{max}) \times 100\% \quad (3)$$

A higher value of  $\eta$  indicates a more uniform electric field distribution. Therefore, this parameter was used to compare the effectiveness of the homogeneous, SB-type, and BS-type configurations in achieving electric field leveling [6], [9].

## 2.5. Data Processing and Comparative Analysis

The electric field data obtained from the simulation were processed into two forms of result presentation. First, the radial electric field profiles of the three configurations were plotted in a graph of electric field magnitude versus radial distance. This graph was used to visualize the difference in field concentration behavior among the homogeneous, SB-type FGM, and BS-type FGM structures. Second, the characteristic parameters  $E_{max}$ ,  $E_{min}$ ,  $E_{avg}$ , and  $\eta$  were summarized in a comparison table to support quantitative analysis.

The homogeneous insulator was used as the reference configuration. The SB-type and BS-type FGM configurations were then compared with the homogeneous model in terms of their ability to reduce the maximum electric field and improve the field grading index. The optimum FGM configuration was identified based on the lowest  $E_{max}$  and the highest  $\eta$ .

## 3. Results and Discussions

### 3.1. Electric Field Characteristics of the Homogeneous Insulator

The homogeneous solid insulator was used as the reference configuration to evaluate the effectiveness of the FGM-based field grading approach. Under the applied voltage of 150 kV, the electric field distribution along the radial direction was found to be non-uniform, with the highest electric field occurring near the inner side of the insulator adjacent to the high-voltage conductor. This result indicates that the homogeneous dielectric structure is unable to redistribute the electric field effectively, leading to field concentration in the critical region.

Based on the simulation result, the homogeneous insulator produced a maximum electric field of 5.099 kV/mm, a minimum electric field of 1.911 kV/mm, and an average electric field of 3.000 kV/mm. The corresponding electric field grading index was 58.85%. These values show that although the homogeneous structure provides a moderate electric field profile, the field distribution is still insufficiently uniform, and the peak field remains relatively high. Therefore, the homogeneous insulator serves as an appropriate baseline for assessing the improvement achieved by the FGM configurations.

### 3.2. Comparison of Electric Field Distribution Profiles

Figure 2 shows the radial electric field distribution of the homogeneous insulator, SB-type FGM, and BS-type FGM under the applied voltage of 150 kV. The graph clearly indicates that the three dielectric configurations produce different electric field profiles. The SB-type FGM exhibits the highest electric field peak near the inner radial region, followed by the homogeneous insulator, while the BS-type FGM shows the lowest peak electric field among all configurations. This result confirms that the direction of permittivity grading strongly influences the redistribution of electric field intensity inside the insulator.

In the SB-type configuration, the electric field sharply increases near the high-voltage side, indicating that the adopted grading direction is unfavorable for suppressing field concentration. In contrast, the BS-type FGM produces a flatter radial field profile, indicating a more effective redistribution of the electric field from the highly stressed region to the surrounding dielectric layers.

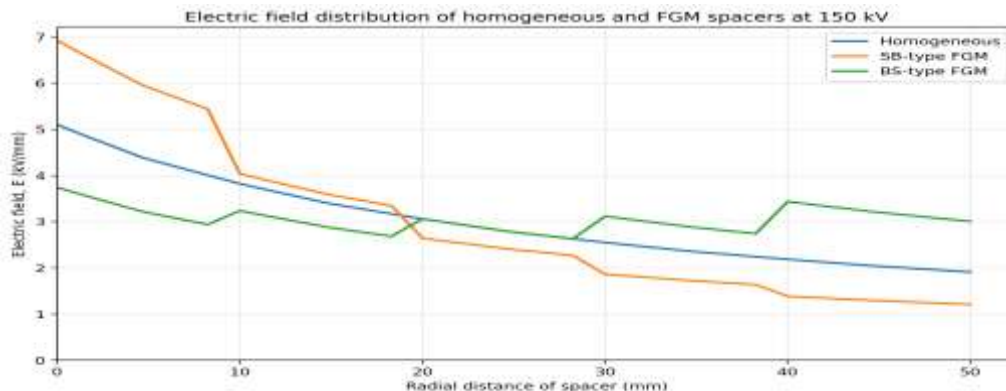


Figure 2. Electric field distribution of homogeneous and FGM solid insulators at 150 kV.

To further examine the field enhancement behavior in the critical regions, two pairwise comparisons were prepared between the homogeneous spacer and each FGM configuration. These plots provide a clearer view of the electric field redistribution at the inner triple-junction near the high-voltage conductor (TJ-HV) and at the outer triple-junction near the grounded side (TJ-GND).

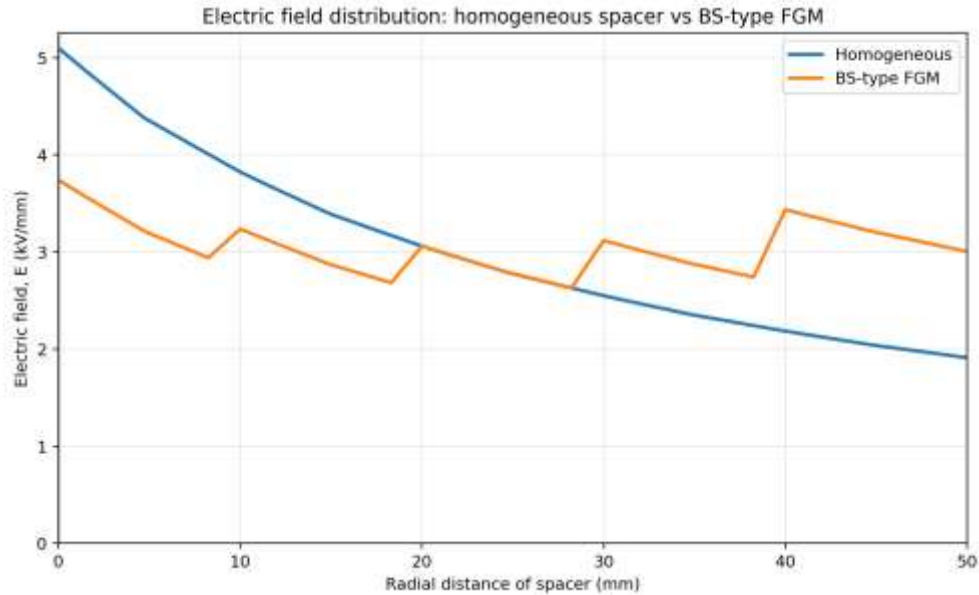


Figure 3. Comparison of radial electric field distribution between the homogeneous spacer and the BS-type FGM spacer at 150 kV.

Figure 3 shows that the BS-type FGM significantly suppresses local field enhancement in the TJ-HV region. At the inner critical region, the electric field decreases from 5.099 kV/mm for the homogeneous spacer to 3.741 kV/mm for the BS-type FGM, corresponding to a reduction of approximately 26.63%. In contrast, at the outer region near TJ-GND, the electric field increases from 1.911 kV/mm to 3.004 kV/mm. This behavior indicates that the BS-type permittivity grading redistributes the electric field away from the highly stressed TJ-HV region toward the outer dielectric region, resulting in a flatter radial profile and improved field grading performance.

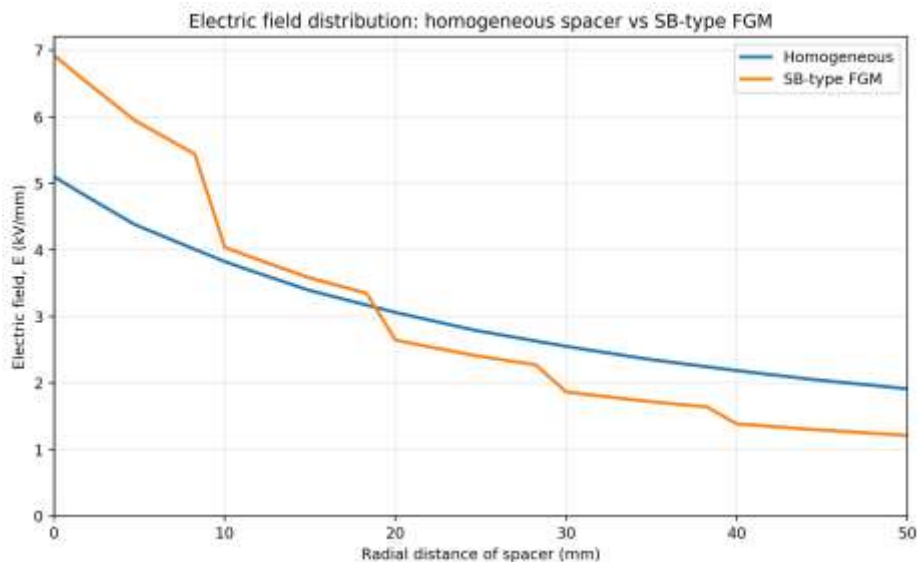


Figure 4. Comparison of radial electric field distribution between the homogeneous spacer and the SB-type FGM spacer at 150 kV.

Figure 4 indicates that the SB-type FGM intensifies local field enhancement in the TJ-HV region. The electric field at TJ-HV increases from 5.099 kV/mm for the homogeneous spacer to 6.921 kV/mm for the SB-type FGM, which corresponds to an increase of about 35.74%. Meanwhile, the electric field near TJ-GND decreases from 1.911 kV/mm to 1.210 kV/mm. This result confirms that the SB-type permittivity arrangement shifts the electric field concentration toward the inner critical region instead of reducing it. Therefore, the SB-type FGM is unfavorable for electric field leveling because it intensifies the local electric stress at TJ-HV.

These pairwise comparisons confirm that the direction of permittivity grading strongly affects the local field enhancement behavior. The BS-type FGM mitigates the field enhancement at TJ-HV and redistributes the electric field more evenly toward the outer region, whereas the SB-type FGM causes excessive field concentration near the high-voltage side.

### 3.3. Characteristic Parameters of Electric Field Distribution

To quantify the differences among the three configurations, the characteristic parameters of electric field distribution are summarized in Table 2.

Table 2. Electric field characteristic parameters of homogeneous and FGM solid insulators.

Insulator Type	$E_{max}$ (kV/mm)	$E_{min}$ (kV/mm)	$E_{avg}$ (kV/mm)	Grading Index, $\eta$ (%)
Homogeneous	5.099	1.911	3.000	58.85
SB-type FGM	6.921	1.210	2.960	42.78
BS-type FGM	3.741	2.630	3.039	81.25

From Table 2, it can be observed that the BS-type FGM achieved the best performance. The maximum electric field of the BS-type FGM was 3.741 kV/mm, which is significantly lower than that of the homogeneous insulator at 5.099 kV/mm and the SB-type FGM at 6.921 kV/mm. This means that the BS-type configuration successfully reduced the peak electric field by approximately 26.63% compared with the homogeneous insulator.

Meanwhile, the SB-type FGM produced the worst result, with the highest maximum electric field among all configurations. Compared with the homogeneous insulator, the maximum electric field of the SB-type increased by approximately 35.74%. This indicates that not all permittivity grading arrangements are beneficial, and the effectiveness of FGM strongly depends on the direction of dielectric grading.

### 3.4. Electric Field Grading Performance

The electric field grading index,  $\eta$ , was used to evaluate the uniformity of the electric field distribution. A larger value of  $\eta$  indicates that the average electric field is closer to the maximum electric field, which means the field distribution is more uniform.

The BS-type FGM achieved the highest grading index of 81.25%, followed by the homogeneous insulator with 58.85%, and the SB-type FGM with 42.78%. These results show that the BS-type FGM provided the most uniform electric field distribution, whereas the SB-type FGM resulted in the poorest field uniformity. Therefore, from the viewpoint of electric field grading performance, the BS-type FGM can be considered the optimum configuration among the three models investigated in this study.

### 3.5. Implications for Insulation Performance

The reduction of maximum electric field in the critical region is important because high local electric stress is closely associated with insulation deterioration and the initiation of local electrical discharges. In practical applications, a lower  $E_{max}$  implies a better electrical margin and a lower probability of stress-induced insulation failure.

When the simulation results are compared with common dielectric strength references, the homogeneous insulator and the SB-type FGM produce electric field peaks above 3 kV/mm, which is often used as a general reference for

air insulation. The BS-type FGM also remains slightly above this value, but it still provides the lowest electric field severity among all configurations. For SF6-based insulation, using a general dielectric strength reference of 8.9 kV/mm, all three configurations remain below the limit. Therefore, although this study does not include direct partial discharge or breakdown testing, the numerical results indicate that the BS-type FGM has the greatest potential for improving insulation performance by suppressing electric field concentration in critical regions.

#### 4. Conclusion

This study investigated the electric field characteristics of homogeneous and functionally graded material (FGM) solid insulators using a numerical simulation approach. Three dielectric configurations were evaluated, namely homogeneous insulation, SB-type FGM, and BS-type FGM, in a cylindrical coaxial geometry under an applied voltage of 150 kV. The results demonstrated that the permittivity distribution has a significant effect on electric field behavior inside the solid insulator. Among the investigated configurations, the BS-type FGM showed the best performance by producing the lowest maximum electric field of 3.741 kV/mm and the highest electric field grading index of 81.25%. In contrast, the SB-type FGM resulted in the highest field concentration and the lowest grading performance. These findings indicate that the BS-type permittivity arrangement is the most effective configuration for reducing electric field concentration and improving field uniformity in critical regions. Therefore, numerical simulation can be considered an effective approach for optimizing the design of FGM solid insulators and for identifying dielectric grading schemes with better insulation performance.

#### Reference

- [1] Rachmawati, H. Kojima, N. Hayakawa, K. Kato, and N. Zebouchi, "Electric Field Simulation of Permittivity and Conductivity Graded Materials ( $\epsilon/\sigma$ -FGM) for HVDC GIS Spacers," *IEEE Transactions on Dielectrics and Electrical Insulation*, vol. 28, no. 2, pp. 736–744, Apr. 2021, doi: 10.1109/TDEI.2020.009343.
- [2] N. Hayakawa, K. Kato, M. Hikita, H. Okubo, K. Watanabe, K. Adachi, and K. Okamoto, "Development of Cone-Type FGM Spacer for Actual Size GIS," in 2020 IEEE Conference on Electrical Insulation and Dielectric Phenomena (CEIDP), 2020, pp. 255–258, doi: 10.1109/CEIDP49254.2020.9437434.
- [3] Rachmawati, A. Izu, R. Nakane, H. Kojima, K. Kato, N. Zebouchi, and N. Hayakawa, "Electric Field Grading by Permittivity and Conductivity Graded Materials ( $\epsilon/\sigma$ -FGM) for HVDC Gas Insulated Power Apparatus," in *Proceedings of the 9th International Symposium on Electrical Insulating Materials (ISEIM)*, 2020, pp. 421–424.
- [4] Y. Miyazaki, A. Izu, Z. Liang, H. Kojima, H. Masui, H. Mitsudome, H. Yanase, K. Okamoto, K. Watanabe, K. Kato, and N. Hayakawa, "Breakdown Characteristics of Cone-type  $\epsilon$ -FGM Spacer for Gas Insulated Switchgears," in *Proceedings of the International Symposium on Electrical Insulating Materials (ISEIM)*, 2020, pp. 533–536.
- [5] U. Khayam, Rachmawati, S. Hidayat, and F. Damanik, "Effect of Spacer Insulation Material Permittivity on the Electric Field of 150 kV Three-Phase GIS Spacer," in 2019 2nd International Conference on High Voltage Engineering and Power Systems (ICHVEPS), Bali, Indonesia, 2019, pp. 291–296.
- [6] J. Ishiguro, M. Kurimoto, H. Kojima, K. Kato, H. Okubo, and N. Hayakawa, "Electric Field Control in Coaxial Disk-Type Solid Insulator by Functionally Graded Materials (FGM)," in 2014 Annual Report Conference on Electrical Insulation and Dielectric Phenomena, 2014, pp. 663–666.
- [7] M. Kurimoto, A. Kai, K. Kato, and H. Okubo, "Fabrication of Permittivity Graded Materials for Reducing Electric Stress on Electrode Surface," in 2008 IEEE Conference on Electrical Insulation and Dielectric Phenomena, 2008, pp. 265–268.
- [8] K. Ochiai, A. Izu, R. Oishi, H. Kojima, H. Mitsudome, H. Yanase, K. Okamoto, K. Kato, and N. Hayakawa, "Fabrication of Permittivity Graded Materials ( $\epsilon$ -FGM) by Flexible Mixture Casting Method," in 2018 IEEE Conference on Electrical Insulation and Dielectric Phenomena (CEIDP), 2018, pp. 578–581.
- [9] G. M. Naik, J. Amamath, S. Kamakshiah, and G. Sai Srujana, "Computation of Electric Field for FGM Spacer Using U-Shape Insulator in GIS," in 2012 Annual Report Conference on Electrical Insulation and Dielectric Phenomena, 2012.
- [10] S. Hidayat, F. Damanik, and U. Khayam, "Electric Field Optimization on 150 kV GIS Spacer by Modification of Spacer Shape and Conductor Configuration," in 2016 3rd International Conference on Information Technology, Computer, and Electrical Engineering (ICITACEE), 2016.
- [11] R. Oishi, A. Izu, H. Kojima, K. Kato, and N. Hayakawa, "Electric Field Relaxation of Functionally Graded Material Spacer," in *Proceedings of the International Symposium on High Voltage Engineering (ISH)*, 2017, paper OG1-3.
- [12] M. Talaat, A. El-Zein, and M. Amin, "Electric Field Simulation for Uniform and FGM Cone Type Spacer with Adhering Spherical Conducting Particle," *IEEE Transactions on Dielectrics and Electrical Insulation*, vol. 25, no. 1, pp. 347–350, Feb. 2018.
- [13] S. A. Qasim and N. Gupta, "Functionally Graded Material Composites for Effective Stress Control in Insulators," in 2015 IEEE 11th International Conference on the Properties and Applications of Dielectric Materials (ICPADM), 2015, pp. 232–235.
- [14] M. Kurimoto, Y. Yamashita, T. Yoshida, H. Ozaki, Y. Manabe, T. Funabashi, T. Kato, and Y. Suzuoki, "Influence of Nanopore Diameter on Dielectric Permittivity of Epoxy/Open Nanoporous Silica Microcomposites," *IEEE Transactions on Dielectrics and Electrical Insulation*, vol. 25, no. 3, pp. 1023–1030, Jun. 2018.
- [15] M. Pradhan, H. Greijer, G. Eriksson, and M. Unge, "Functional Behaviors of Electric Field Grading Composite Materials," *IEEE Transactions on Dielectrics and Electrical Insulation*, vol. 22, no. 2, pp. 768–776, Apr. 2015, doi: 10.1109/TDEI.2015.005288.